

# The Tropospheric Jet Response to Prescribed Zonal Forcing in an Idealized Atmospheric Model

GANG CHEN

*Program in Atmospheres, Oceans and Climate, Massachusetts Institute of Technology, Cambridge, Massachusetts*

PABLO ZURITA-GOTOR

*Universidad Complutense de Madrid, Madrid, Spain*

(Manuscript received 14 August 2007, in final form 19 November 2007)

## ABSTRACT

This paper explores the tropospheric jet shift to a prescribed zonal torque in an idealized dry atmospheric model with high stratospheric resolution. The jet moves in opposite directions for torques on the jet's equatorward and poleward flanks in the troposphere. This can be explained by considering how the critical latitudes for wave activity absorption change, where the eastward propagation speed of eddies equals the background zonal mean zonal wind. While the increased zonal winds in the subtropics allow the midlatitude eddies to propagate farther into the tropics and result in the equatorward shift in the critical latitudes, the increased winds in the midlatitudes accelerate the eastward eddy phase speeds and lead to the poleward shift in the critical latitudes.

In contrast, the jet moves poleward when a westerly torque is placed in the extratropical stratosphere irrespective of the forcing latitude. The downward penetration of zonal winds to the troposphere displays a poleward slope for the subtropical torque, an equatorward slope for the high-latitude torque, and less tilting for the midlatitude torques. The stratospheric eddies play a key role in transferring zonal wind anomalies downward into the troposphere. It is argued that these stratospheric zonal wind anomalies can affect the tropospheric jet by altering the eastward propagation of tropospheric eddies. Additionally, the zonal wind response to a subtropical zonal torque in this idealized model is of value in understanding the tropospheric jet sensitivity to the orographic gravity wave drag parameterization in a realistic climate model.

## 1. Introduction

Recent observational studies suggest that variability in the stratospheric flow has a substantial influence on the tropospheric circulation on various time scales. On the time scale of several weeks or months, large anomalies in the strength of the stratospheric polar jet are followed by similar-signed anomalies in the tropospheric annular mode that can persist for up to 2 months in both hemispheres (Baldwin and Dunkerton 1999, 2001; Thompson et al. 2005). In the long-term climate trend, the poleward shift of the Southern Hemisphere surface westerlies in recent decades has been attributed in part to the strengthening of the strato-

spheric polar vortex because of ozone depletion (e.g., Thompson and Solomon 2002; Chen and Held 2007).

The stratospheric influence on the troposphere is also found in model simulations. The persistence and the trend of the Northern Hemisphere annular mode in a climate model can be strongly affected by the stratospheric polar vortex (Norton 2003; Scaife et al. 2005). Despite the differences in model details and experiment designs, a number of idealized models have generated a consistent downward influence of the stratosphere: as the subpolar stratospheric zonal winds are increased, the tropospheric jet displaces poleward, and this poleward displacement projects strongly onto the leading mode of the intrinsic variability in the troposphere (Polvani and Kushner 2002; Taguchi 2003; Song and Robinson 2004; Kushner and Polvani 2004; Haigh et al. 2005).

However, the mechanism through which increased lower-stratospheric winds shift the tropospheric jet re-

---

*Corresponding author address:* Gang Chen, Program in Atmospheres, Oceans and Climate, Massachusetts Institute of Technology, Cambridge, MA 02139.  
E-mail: gchenpu@mit.edu

mains obscure. Previous studies have mainly focused on the effects of the eddy-induced zonal forcings and the vertical wind shears in the lower stratosphere. These zonal forcings can induce a meridional residual circulation that extends downward and closes in the planetary boundary layer. This provides a zonally symmetric pathway to redistribute momentum in the vertical, generally referred to as “downward control” (Haynes et al. 1991). On the other hand, changes in the stratospheric wind shear can either affect the vertical propagation and reflection of planetary waves (e.g., Chen and Robinson 1992; Perlwitz and Harnik 2003), or modify baroclinic eddy life cycles in the troposphere (Wittman et al. 2007). But to generate a jet shift with a deep annular mode-like structure, the tropospheric eddies must be modified (Kushner and Polvani 2004; Song and Robinson 2004). This can also be seen in Thompson et al. (2006), in which the residual circulation forced by the stratospheric eddies extends to the surface but zonal wind changes decrease rapidly downward from the level of forcing.

Central to the tropospheric jet shift is the eddy momentum flux, which, in the zonal momentum balance, drives the barotropic component of the zonal wind against the frictional damping near the surface. The eddy momentum flux diverges from the subtropics into the midlatitude jet in the upper troposphere, as the midlatitude eddies propagate equatorward and get absorbed near their subtropical critical latitudes, where the eddy phase speed equals the background zonal mean wind [see Held and Phillips (1987) for a simple example]. In a tropospheric model, the midlatitude jet is displaced poleward as the strength of the surface friction is reduced (Robinson 1997), and Chen et al. (2007, hereafter CHR) argue that the increased eastward propagation of midlatitude eddies due to the zonal wind acceleration plays a key role in generating this poleward shift. It is then natural to ask whether increased lower-stratospheric winds may affect tropospheric eddies in the same way. CHR show that the response to changes in surface friction can be approximated by prescribing the zonal torque associated with anomalous winds at the surface. This suggests that one may be able to relate both problems by considering how the atmospheric response to a prescribed zonal torque changes when the torque location is moved up across the troposphere and into the stratosphere.

In this paper, we study the atmospheric response to a prescribed zonal torque in a systematic manner. We first examine the process that gives rise to the tropospheric jet shift when a zonal torque is applied in the troposphere, and then explore the stratospheric influence on the tropospheric jet with a zonal torque in the

stratosphere. Our work follows up on previous studies by Song and Robinson (2004, hereafter SR) and Ring and Plumb (2007, hereafter RP), who argue that one can think of the tropospheric annular mode as an internal mode arising from the tropospheric eddy dynamics. The response to external forcing can then be understood in terms of the projection of this forcing (or its downward extension, for the stratospheric case) on the internal mode. Our goal is to investigate the dynamical mechanisms linking the external tropospheric or stratospheric forcing and the internal mode response in the troposphere, and in particular whether changes in the eddy phase speed and subtropical critical layer may be important for the jet shift, which would be similar to the case when friction is varied.

This study is also motivated by an attempt to understand the model sensitivity when tuning the orographic gravity wave drag (GWD) in climate models. While the orographic GWD is localized above the steep topography, an adjustment of the GWD profile in the vertical has an impact on the global circulation, including meridional shifts of the midlatitude jet (e.g., Stephenson 1994). To the extent that the zonal mean response is mainly caused by the GWD on the zonal mean flow, it is of value to examine the jet sensitivity to the vertical level of a zonal torque imposed in a simple model.

We use the idealized dry model described in Held and Suarez (1994) with enhanced stratospheric resolution. In contrast to previous model studies on stratosphere–troposphere coupling, this model does not have a stratospheric polar jet. As a result, this configuration minimizes the stratospheric intrinsic variability and its influence on the troposphere in the control simulation, making it easier to isolate the dynamical processes responsible for the model’s response to the external forcing. As we shall see, the forced response in this model is similar to that in models with a stratospheric polar jet, which suggests that the insights that we obtain here may still be relevant with a more active stratosphere and stratosphere–troposphere coupling.

The paper is organized as follows. We first describe the characteristics of the idealized dry model and control simulation in section 2. Then, we study the sensitivity of the tropospheric jet latitude when the location of the zonal torque is varied in section 3. Next, we examine the processes that give rise to the tropospheric jet shift for a tropospheric torque in section 4, and for a stratospheric torque in section 5. Our aim is to separate the direct response to the external forcings from the projection onto the tropospheric internal variability. In section 6, we discuss the implications of our results for the jet sensitivity to the orographic GWD pa-

parameterization in a realistic climate model. Finally, we provide a brief summary and discussion in section 7.

## 2. The idealized dry model

### a. The model configuration

We employ the Geophysical Fluid Dynamics Laboratory (GFDL) spectral atmospheric dynamical core. The model uses a sigma vertical coordinate, with the vertical differencing scheme described in Simmons and Burridge (1981). The sigma value on the  $k$ th half-level  $\sigma_{k+1/2}$  is defined by the following profile so as to attain a high resolution in the stratosphere:

$$\sigma_{k+1/2} = \exp[-\gamma(1 - k/N)^\alpha], \quad \text{for } k = 0, \dots, N, \quad (1)$$

where  $N$  is the total number of model levels, and  $\gamma$  and  $\alpha$  are two constants. The values of  $\gamma$  and  $\alpha$  are obtained by specifying the model upper boundary as  $\sigma_{1/2} = \exp(-\gamma) = 1 \times 10^{-5}$  and the median vertical level as  $\sigma_{N/2+1/2} = \exp(-\gamma 0.5^\alpha) = 0.1$ . As a result, about half of the model levels lie in the stratosphere.

A sponge layer is applied in the top model levels to prevent artificial wave reflection at the upper boundary. Following Scott and Polvani (2006), we use linear Rayleigh damping only on the eddies in the momentum equations, as the damping on the zonal mean flow may induce an unwanted downward influence. The damping coefficient is specified as  $\kappa_{\text{sp}}[(\sigma_{\text{sp}} - \sigma)/\sigma_{\text{sp}}]^2$  (for  $\sigma < \sigma_{\text{sp}}$ ), in which the lowest level of the sponge layer is  $\sigma_{\text{sp}} = 5 \times 10^{-4}$ , and the maximum damping rate is  $\kappa_{\text{sp}}^{-1} = 0.5$  days.

The model is forced by zonally symmetric Newtonian relaxation to the prescribed equilibrium temperature field, which is isothermal in the stratosphere and damped by Rayleigh friction near the surface, as in Held and Suarez (1994). Since the model uses a flat lower boundary, there are no stationary planetary waves, but instantaneous planetary waves exist and are important for propagating the stratospheric signal downward. The hyperdiffusion ( $\nabla^8$ ) is set so that the diffusive damping time of the smallest retained spherical harmonic is 0.1 days. The model is run with T42 horizontal resolution and 40 vertical levels. The model output is sampled daily, and the results presented are averaged over the last 5200 days of 6000-day integrations. In all of the simulations, the forcings and dampings are hemispherically symmetric, and the similarity between the climatologies in both hemispheres confirms the robustness of our results.

### b. The control simulation

Figure 1 shows the time and zonally averaged zonal wind, and the regressions of the zonally averaged zonal wind and Eliassen–Palm (EP) flux divergence anomalies on the standardized annular mode index in the control experiment. The annular mode index here is defined as the first principal component of the zonally and daily averaged surface pressure in one hemisphere. The climatological mean zonal wind displays a tropospheric jet with maximum wind at about  $40^\circ$  latitude and sigma level  $\sigma = 0.25$ . The regression maps show that the midlatitude jet vacillates about this mean latitude with anomalous westerlies at  $50^\circ$  and easterlies at  $30^\circ$ , associated with anomalous baroclinic eddy generation near the surface and anomalous meridional wave propagation in the upper troposphere. The extratropical winds in the stratosphere are weak in the climatological mean and display relatively little variability, as expected from the isothermal radiative equilibrium temperature in the stratosphere. The EP vector regression map indicates anomalous upward wave activity flux into the midlatitude lower stratosphere, and anomalous downward flux into the subtropical upper troposphere. In comparison with the statistics in Held and Suarez (1994), the mean tropospheric jet in this model is shifted slightly equatorward, and the low-frequency jet vacillation is much more persistent, as was also found by Gerber et al. (2008).

We describe eddy characteristics with the phase speed spectrum introduced by Randel and Held (1991). The 5200-day time series is divided into 13 segments of length  $T = 400$  days and tapered by a Hanning window. For each segment, wavenumber–frequency spectra are calculated and then converted to wavenumber–angular phase speed space. In the figures, we use angular phase speeds multiplied by the earth’s radius (phase speeds divided by  $\cos \theta$ ) for comparison with zonal winds. The resolution in angular phase speed space  $\Delta c_A$  is limited by the time period  $T$  and zonal wavenumber  $m$ ,  $\Delta c_A = a(2\pi/T)/m$  (where  $a$  is the earth’s radius). Since the troposphere is dominated by medium-scale eddies ( $4 \leq m \leq 7$ ) in the model, we neglect the small contribution of  $m = 1$  to the spectra.

Figure 2 shows the eddy momentum flux convergence in the upper troposphere ( $\sigma = 0.230$ ) and eddy heat flux in the lower troposphere ( $\sigma = 0.843$ ) as a function of latitude and angular phase speed in the control experiment. The figure displays the familiar eddy momentum flux divergence slightly poleward of the subtropical critical latitudes and momentum flux convergence into the midlatitude jet in the upper troposphere, as well as the poleward heat flux in the lower

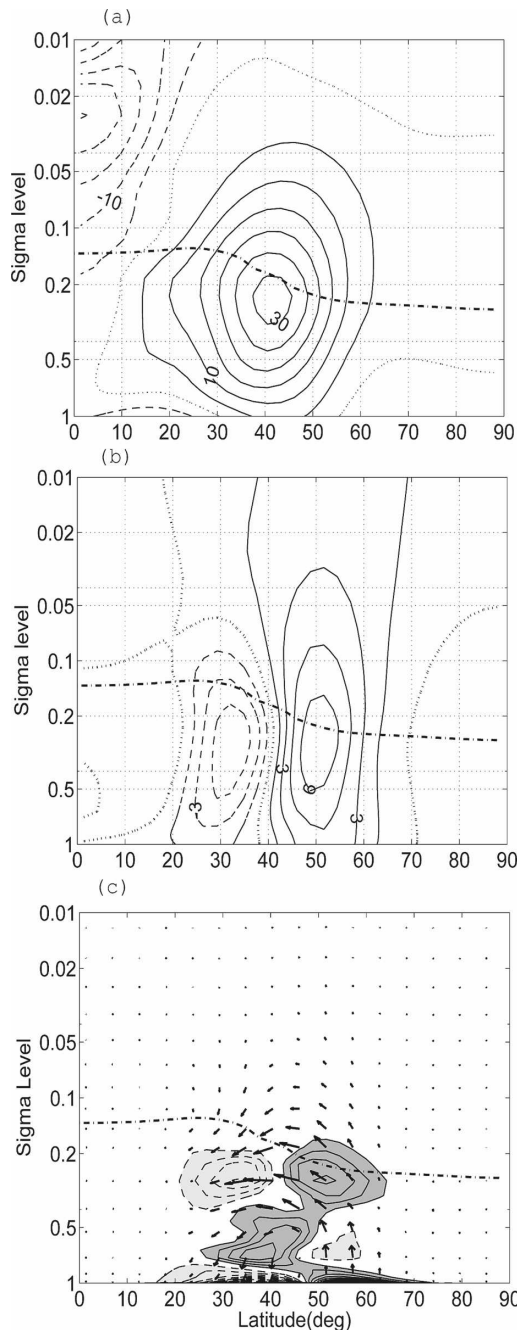


FIG. 1. For the control simulation, (a) the time and zonally averaged zonal wind and the regressions of (b) the zonally averaged zonal wind and of (c) the EP flux divergence anomalies on the standardized annular mode index. The dashed-dotted lines in the plots are the tropopause level, estimated by the standard World Meteorological Organization (WMO) lapse rate criterion. The contour intervals are  $5 \text{ m s}^{-1}$  for (a),  $1.5 \text{ m s}^{-1}$  for (b), and  $0.5 \text{ m s}^{-1} \text{ day}^{-1}$  for (c). The dark (light) shading in (c) denotes the EP flux divergence (convergence). The EP vectors in (c) denote wave activity fluxes of  $4 \text{ m s}^{-1} \text{ day}^{-1} \times (\Delta\sigma, \Delta\phi)$  [where  $(\Delta\sigma, \Delta\phi)$  are the lengths of the vectors projected on the vertical level and latitude, respectively], and the vectors are plotted on selected grid points representative of the wave activity pattern.

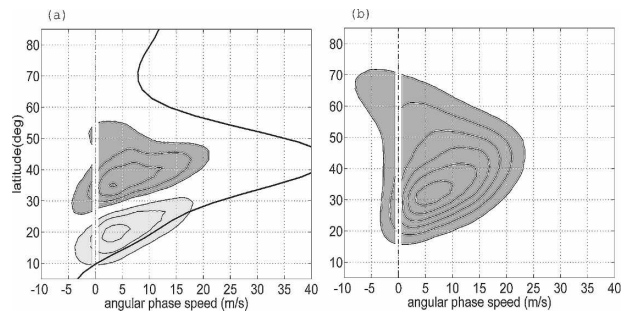


FIG. 2. For the control simulation, (a) the eddy momentum flux convergence in the upper troposphere ( $\sigma = 0.230$ ) and (b) the eddy heat flux in the lower troposphere ( $\sigma = 0.843$ ) as a function of latitude and angular phase speed. The thick solid line in (a) is the time and zonally averaged zonal wind at  $\sigma = 0.230$ , divided by  $\cos \phi$  for comparison. The contour intervals are  $0.03 \text{ m s}^{-1} \text{ day}^{-1}$  for (a) and  $0.08 \text{ K m s}^{-1}$  for (b). The dark (light) shading denotes positive (negative) values.

troposphere. Both the momentum and heat fluxes are dominated by eddies with angular phase speeds between  $0$  and  $10 \text{ m s}^{-1}$ , with a peak around  $5 \text{ m s}^{-1}$ . A key feature is that the absorption of upper-tropospheric eddies in the subtropics is confined within a critical layer of  $10^\circ$ – $20^\circ$  in latitude poleward of their linear critical latitudes, and therefore the movement of the critical latitudes is useful to understand the latitudinal movement of eddy momentum fluxes and the eddy-driven jet, as in CHR.

### 3. A sensitivity study

In this section, we examine the sensitivity of the tropospheric jet latitude to a time-independent and zonally symmetric zonal torque. The zonal torque that we impose is identical in both hemispheres, in contrast to the dipolar structure used in SR and RP. This introduces an angular momentum source to the model, which is eventually removed by surface friction in the same hemisphere. Hence, it is not necessary to impose an angular momentum source in one hemisphere and a sink in the other. The zonal torque  $T$  has the following form:

$$\begin{aligned}
 T &= A_0 G(\phi) \cos[\eta(\sigma)\pi] \quad \text{for} \\
 &-0.5 \leq \eta(\sigma) \leq 0.5, \quad \text{and} \\
 &= 0 \quad \text{elsewhere,} \quad (2)
 \end{aligned}$$

where  $A_0$  is the forcing amplitude. When the amplitude of  $A_0$  is increased or the sign is changed, the tropospheric response is fairly linear, as is also seen in SR and RP. Therefore, we focus on the jet response to the location of a westerly (eastward) torque with fixed am-

plitude  $A_0 = 2 \text{ m s}^{-1} \text{ day}^{-1}$ , which generates a zonal wind response of comparable magnitude to the internal wind variability in the model. Here,  $G(\phi)$  controls the meridional structure of the torque and consists of a Gaussian function with its maximum at the forcing latitude  $\phi_0$  and meridional half-width  $\phi_w = 9^\circ$ . The factor  $\cos[\eta(\sigma)\pi]$  controls the vertical structure, in which  $\eta(\sigma)$  is centered at the forcing level  $\sigma_0$ , with a linear vertical profile when  $\sigma_0$  is below the sigma level 0.3, and with a logarithmic profile when  $\sigma_0$  is above this level:

$$\eta(\sigma) = (\sigma_0 - \sigma)/\sigma_w \quad \text{for } \sigma_0 \geq 0.3, \quad \sigma_w = 0.3, \quad \text{and} \\ = (\log_{10}\sigma_0 - \log_{10}\sigma)/e_w$$

$$\text{for } \sigma_0 \leq 0.3, \quad e_w = 1.0. \quad (3)$$

We perform a comprehensive sensitivity study with respect to the location of the torque ( $\phi_0, \sigma_0$ ). Most experiments display a tropospheric jet shift similar in structure to the tropospheric annular mode (e.g., Figs. 4 and 9). Therefore, we describe the jet shift succinctly by regressing the zonal wind change  $\delta U(\phi, \sigma)$ , in a least square manner, to the internal annular mode pattern  $U_{AM}(\phi, \sigma)$  shown in Fig. 1b:

$$\delta U(\phi, \sigma) = \beta U_{AM}(\phi, \sigma) + \epsilon, \quad (4)$$

where  $\epsilon$  is the residual of a linear regression, and  $\delta U$  and  $U_{AM}$  are mass weighted at each latitude and sigma level before the regression. The regression coefficient  $\beta$  represents the forced jet movement relative to the internal jet variability, with the positive (negative) sign indicating a poleward (equatorward) shift. Therefore, when  $\beta = 1$ , the zonal wind response is similar in magnitude to the wind variability associated with one standard deviation of the annular mode index in the control simulation.

Figure 3 shows the jet shift as a function of the forcing location. First, we study the dependence on the forcing level when the torque is placed on either the equatorward ( $\phi_0 = 30$ ) or poleward ( $\phi_0 = 50$ ) flank of the jet center (Fig. 3a). The torque in Fig. 3a is placed on the vertical levels at  $\sigma_0 = 0.85, 0.65, 0.45, 0.1, 0.056, 0.032, 0.01$ , and  $0.003$ . As the torque is moved upward in the troposphere, the annular mode-like response changes relatively little. This result may seem counter-intuitive, as a torque at the surface and in the upper troposphere should have opposite effects on vertical wind shears and baroclinic instability. Moreover, when the torque is on the poleward flank of the jet, the sign of the response also remains unchanged as the torque is moved up into the stratosphere. In contrast, the jet movement reverses in direction near the forcing level  $\sigma = 0.1$  when the torque is located on the jet's equa-

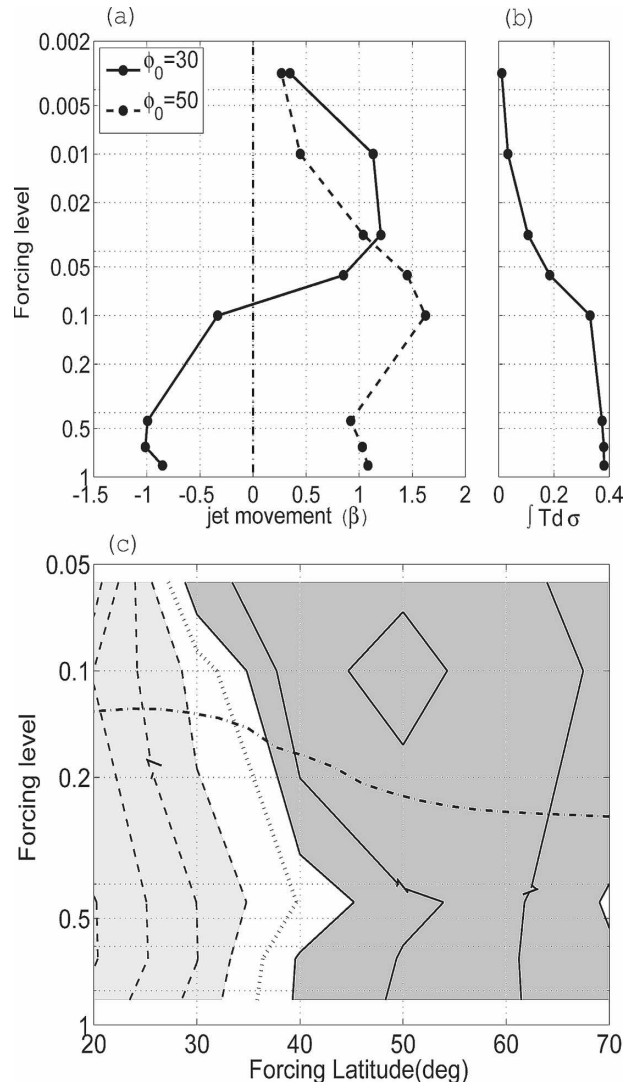


FIG. 3. Sensitivity of the tropospheric jet latitude to the forcing location. The jet movement  $\beta$  is defined in Eq. (4) as the forced jet movement relative to the internal jet variability. (a) Shown is  $\beta$  as a function of the forcing level on the jet's equatorward flank ( $\phi_0 = 30$ ) and poleward flank ( $\phi_0 = 50$ ). (b) The vertical integral of angular momentum added at the forcing latitude,  $\int T d\sigma$ , is shown for reference as a function of the forcing level. (c) Here, we show  $\beta$  as a function of the forcing latitude and the forcing level. The contour intervals greater (less) than 0.5 ( $-0.5$ ) are shaded, and the dark (light) shading denotes a poleward (equatorward) shift. The dashed-dotted line is the tropopause level in the control simulation.

ward flank. In both cases, the tropospheric response eventually becomes negligible when the stratospheric torque is far away from the troposphere.

The vertical integral of the angular momentum added at the forcing latitude  $\int T d\sigma = \int A_0 G(\phi_0) \cos[\eta(\sigma)\pi] d\sigma$  remains roughly constant for the torque in the troposphere and decays exponentially with in-

creasing height for the torque in the stratosphere (Fig. 3b). It is remarkable that the tropospheric jet response is comparable in magnitude when the torque is in the troposphere and in the stratosphere, even though the net momentum added is smaller in the latter case. This suggests that the direct contribution of the zonal torque to the angular momentum balance is not the key for the jet shift, especially for the case of the stratospheric torque.

Next, we look at the response with torque locations in a latitude–sigma level domain below the lower stratosphere (Fig. 3c). The torque is moved in latitude from  $20^\circ$  to  $70^\circ$  in increments of  $10^\circ$ , and on sigma levels at  $\sigma_0 = 0.85, 0.65, 0.45, 0.1$ , and  $0.056$ . (Note that the wind response is very large for the stratospheric torque in the subtropics, and the time step for the model integration is reduced by half to avoid numerical instability.) As the near-surface torque ( $\sigma_0 = 0.85$ ) is moved from low latitudes to high latitudes, the jet response makes the transition from an equatorward shift to a poleward shift near the forcing latitude of  $35^\circ$ . The jet shifts poleward for a westerly torque at the latitude of the surface westerly maximum, consistent with the response to a decrease in surface friction in CHR. As the torque is moved from near the surface to the upper troposphere, the jet response does not change very much except near the jet core. Between the upper troposphere and lower stratosphere, however, the transitional latitude tilts equatorward. In particular, the tropospheric jet shifts poleward for all of the cases in which the torque is placed poleward of  $30^\circ$  in the lower stratosphere ( $\sigma_0 = 0.056$ ).

The internal annular mode explains [in the form of Eq. (4)] at least 60% of the variance for the time and zonally averaged zonal wind change in all but three cases:  $(\phi_0, \sigma_0) = (20^\circ, 0.056)$ ,  $(30^\circ, 0.1)$ , and  $(40^\circ, 0.45)$ . In the first experiment, the imposed torque is mainly balanced by Coriolis deceleration. The small Coriolis parameter in the subtropics results in a very large response in meridional and zonal winds, and eddies play only a minor role. The other two experiments lie on the transition zone from an equatorward to a poleward shift, as the torque is moved across the subtropical tropopause and the jet center, respectively. In the following sections, we study in more detail the dynamics of the response for those experiments in which this response projects well onto the internal annular mode.

#### 4. Response to the tropospheric forcing

We first describe the response when the prescribed tropospheric torque is located near the surface. We

concentrate on two experiments in which the zonal torques ( $\sigma_0 = 0.85$ ) are placed on the equatorward flank ( $\phi = 30^\circ$ ) and poleward flank ( $\phi = 50^\circ$ ) of the jet center. Figure 4 shows the time and zonally averaged changes in the zonal wind and EP flux divergence for both cases. The response displays a large-scale pattern in the zonal wind and wave activity, which is highly correlated with the internal annular mode in both the stratosphere and troposphere, but has the opposite sign for the two cases. Since the wind change shows little resemblance to the external forcing, it is useful to think of the response as a projection onto the internal annular mode as in RP. For the poleward torque case, a westerly wind anomaly is also visible in the subtropical upper troposphere, as the subtropical jet is stronger and more distinctly separated from the eddy-driven jet than in the control climatology.

Eddy feedbacks play a major role for the response displayed in Fig. 4. To show this, we calculate the response to the same prescribed torque in a zonally symmetric model without eddy feedbacks. The model is constructed by making the full model axisymmetric and including the eddy forcings in the control simulation, using the method described in Kushner and Polvani (2004). We integrate the model for 2000 days, and obtain a steady-state solution that matches the control climatology, except in the deep tropics. Figure 5 shows the zonal wind changes in this model for the same surface torques. The zonal wind change displays a fairly barotropic structure from near the surface into the stratosphere, with a slight decrease across the tropopause. The barotropic structure of the zonal wind changes is consistent with downward control theory. As discussed by Robinson (2000), a surface torque can be balanced locally by anomalous surface winds and the associated frictional drag, and thus the torque does not force the interior baroclinicity. It is obvious from Fig. 5 that the response of the symmetric model is very small outside of the forcing regions, which implies that the global annular mode–like response of the full model is primarily driven by eddy feedbacks.

The full model response can thus be thought of as a zonally symmetric balance between the prescribed zonal torque and surface friction at first, followed by the subsequent modifications on the eddies and the eddy-driven zonal flow. However, it is still an open question through which mechanism the original mean flow anomalies lead to the anomalous eddy patterns. It is well known that barotropic shears can modify the nonlinear evolution of baroclinic anomalies, favoring one of two distinct life cycles (LC1 and LC2) (Simmons and Hoskins 1980; Thorncroft et al. 1993; Hartmann

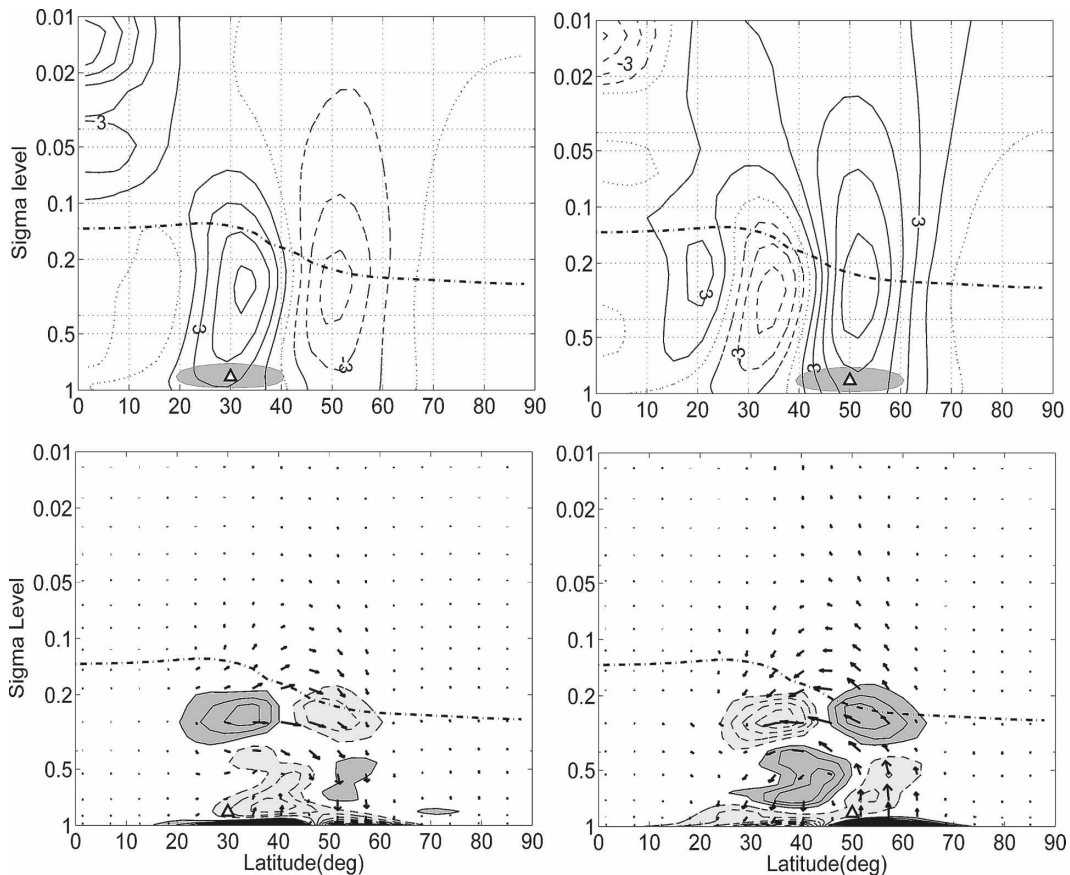


FIG. 4. The time and zonally averaged changes in the (top) zonal wind and (bottom) EP flux divergence, for zonal torques prescribed near the surface ( $\sigma_0 = 0.85$ ) and placed on the jet's (left) equatorward flank ( $\phi_0 = 30$ ) and (right) poleward flank ( $\phi_0 = 50$ ). The triangular symbol denotes the forcing center, and the dark shading in the top panels denotes the region where the torque is greater than  $0.5 \text{ m s}^{-1} \text{ day}^{-1}$ . In the bottom panels, the dark (light) shading denotes the EP flux divergence (convergence). The dashed-dotted lines indicate the tropopause level in the control simulation. The contour intervals are  $1.5 \text{ m s}^{-1}$  for the zonal wind,  $0.5 \text{ m s}^{-1} \text{ day}^{-1}$  for the EP flux divergence, and  $4 \text{ m s}^{-1} \text{ day}^{-1}$  ( $\Delta\sigma$ ,  $\Delta\phi$ ) for the EP vectors.

and Zuercher 1998). In LC1, the wave breaking is primarily on the anticyclonic side of the jet, and the final jet position moves to the poleward flank of the initial jet. In LC2, with enhanced cyclonic shear in the initial condition, waves break on the cyclonic side of the jet, and the jet is displaced slightly equatorward. However, the modification of wave breaking by barotropic shear is a very complex problem, even for a single baroclinic life cycle. On the other hand, CHR have proposed a different mechanism for explaining the jet shift (when friction is varied) that does not depend on changes in the direction of the breaking. These authors show that changes in the eddy phase speed can produce a meridional displacement of the critical layers, leading in turn to a shift of the full eddy pattern. CHR also construct a shallow water model of the upper troposphere in which eddy generation is parameterized as stochastic stirring and show that changes in the phase speed of the pa-

rameterized eddies alone can produce a meridional displacement of the westerlies in that model, even when the barotropic shear does not change.

To investigate whether the phase speed mechanism can also be important in our problem, we have computed the anomalous latitude-phase speed spectra of upper-level eddy momentum flux convergence and lower-level eddy heat flux for the two cases discussed above (Fig. 6). When the torque is located on the poleward flank of the jet (Fig. 6, right panels), the jet displacement is accompanied by an increase in the eddy phase speed in both the eddy momentum flux and eddy heat flux spectra in the midlatitudes. One may thus attribute the jet shift in this case to the poleward displacement of the subtropical critical latitudes when eastward eddy propagation is enhanced by the anomalous westerly advection. This is similar to the transient adjustment following a sudden decrease in surface fric-

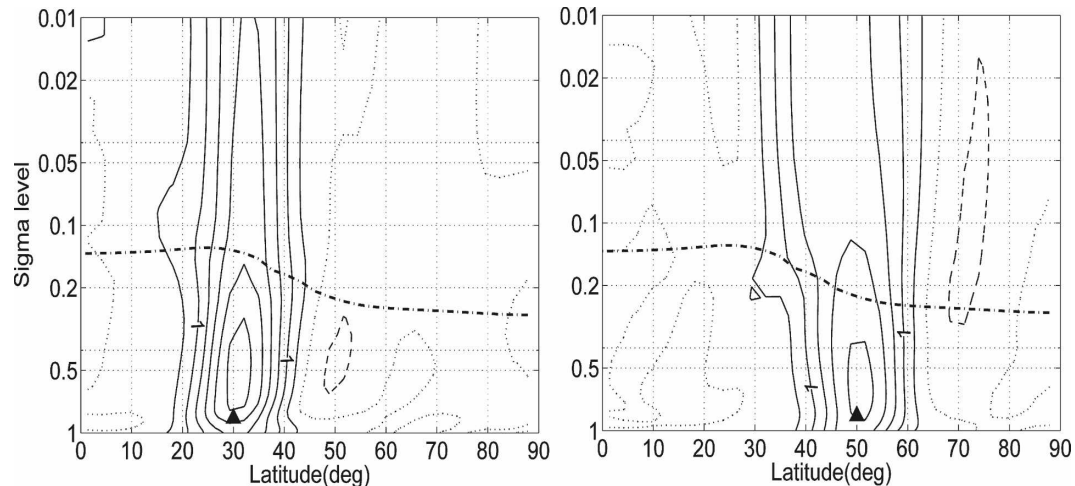


FIG. 5. The zonal wind changes in a zonally symmetric model for the same surface zonal torques in Fig. 4. The triangular symbol denotes the forcing center and the dashed-dotted lines indicate the tropopause level in the control simulation. The contour interval is  $0.5 \text{ m s}^{-1}$ .

tion in CHR. On the other hand, when the torque is located on the equatorward jet flank (Fig. 6, left panels), the subtropical critical latitudes shift equatorward for nearly all phase speeds. The spectra for this case show enhanced eastward propagation in the subtropics, and a slight deceleration in the midlatitudes. However, it is the changes in the mean wind that appear to be more important for the equatorward shift of the critical latitudes and subtropical divergence. The increased zonal wind in the subtropics allows the midlatitude eddies to penetrate farther into the tropics and pushes the subtropical critical latitudes equatorward. This is consistent with the zonal mean extratropical circulation response to the warm phase of the ENSO cycle, during which the increased subtropical winds permit the equatorward shift in the meridional propagation and refraction of Rossby waves (Chang 1995, 1998; Robinson 2002; Seager et al. 2003). As the eddy-driven circulation moves equatorward, the midlatitude eddy phase speeds are also seen to decrease somewhat in the lower-level heat flux spectra, which provides a positive feedback to the equatorward shift.

A nontrivial result is that, in both cases, the response seems to be dominated by “fast” eddies with phase speeds between  $10$  and  $20 \text{ m s}^{-1}$ , rather than by the slower eddies that are more important in the climatology. This occurs because the contributions to the subtropical divergence change from slower eddies are either too small or canceled out in the zonal average. Figure 7 shows the changes in the fluxes as a function of zonal wavenumber and phase speed, area averaged over two latitudinal bands (between  $35^\circ$  and  $45^\circ$  for the eddy momentum flux, and between  $45^\circ$  and  $55^\circ$  for the

eddy heat flux). These bands are chosen to capture the characteristics of the anomalous eddy momentum flux and heat flux maxima associated with the jet movement. The response to a torque on the jet’s poleward flank displays an increase in phase speed in both the momentum flux and heat flux, roughly following the slope of the dispersion relationship in the climatology that smaller eddies propagate faster eastward. However, because there is a cancellation for the dominant climatological eddies ( $m = 5-6$ ) when summing over the zonal wavenumber, the net contribution seen in the latitude–phase speed spectra arises from shorter ( $m = 6-8$ ) and faster eddies. In the case of the subtropical torque, faster eddies also dominate, but the slower eddies change very little. The dominance of fast eddies in the jet movement has also been noted by Son and Lee (2005), when varying the equator-to-pole temperature gradient in a similar model. Attributing the jet response to these fast eddies, we expect the response to change sign as the torque is moving from regions of eddy momentum flux divergence to regions of eddy momentum flux convergence in the climatology. This transition occurs roughly between  $30^\circ$  and  $40^\circ$  for the fast eddies, consistent with Fig. 3c. A zonal torque over this region has little effect because it affects both the zonal mean wind and the eddy phase speed. (Note that there is no jet shift for a surface torque at about  $35^\circ$ , whereas the jet latitude is more like  $40^\circ$ .)

To conclude, we discuss how the results change when the zonal torque is moved up in the troposphere. It is again useful to think of the eddy-free response first. For an interior torque, a mean meridional circulation is required in the symmetric problem to bring down the

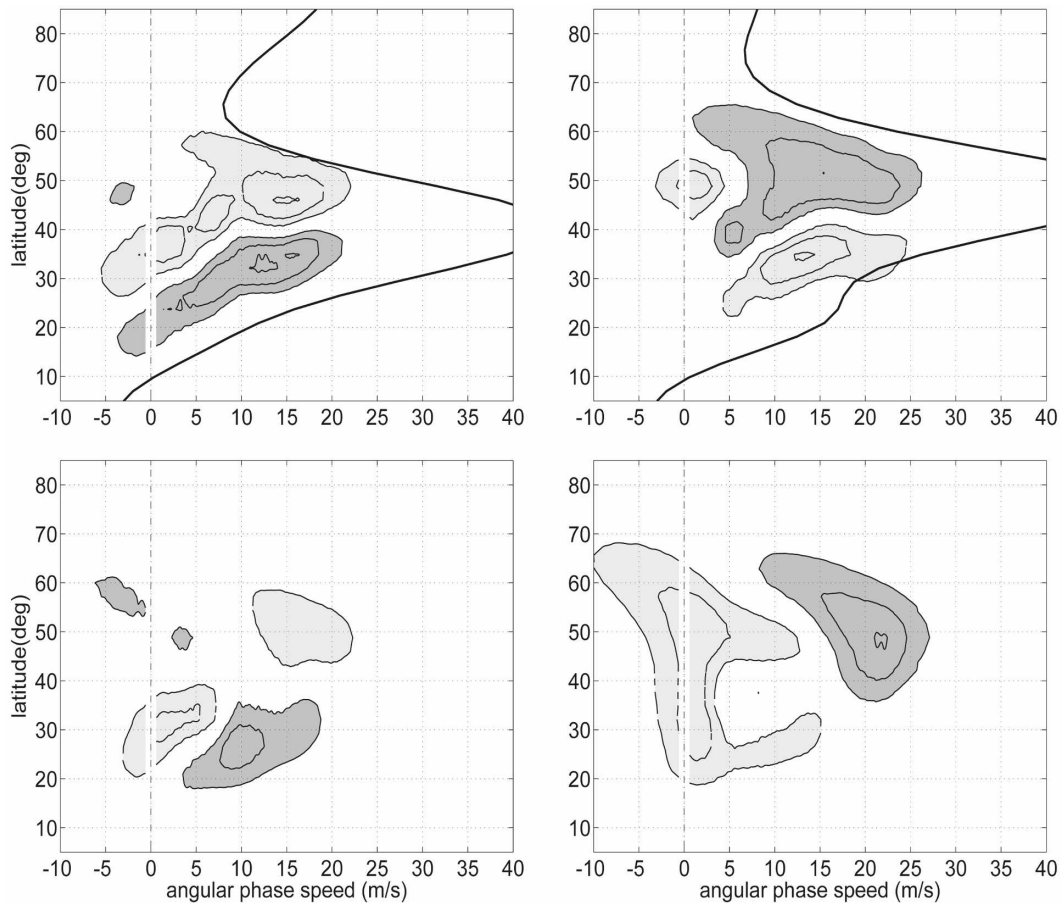


FIG. 6. The changes in the latitude–phase speed spectra of the (top) upper-level ( $\sigma = 0.230$ ) eddy momentum flux convergence and (bottom) lower-level ( $\sigma = 0.843$ ) eddy heat flux, for the same surface torques on the jet’s (left) equatorward flank and (right) poleward flank as in Fig. 4. The thick solid lines in the top panels are the time and zonally averaged upper-level ( $\sigma = 0.230$ ) zonal winds, divided by  $\cos \phi$  for comparison. The contour intervals are  $0.015 \text{ m s}^{-1} \text{ day}^{-1}$  for the momentum flux convergence and  $0.04 \text{ K m s}^{-1}$  for the heat flux. The dark (light) shading denotes positive (negative) values.

momentum forcing to the surface, where it can be balanced by friction. Since this circulation also transports heat, the response of the zonally symmetric model is no longer purely barotropic as for the near-surface torque considered earlier, but the baroclinic wind is also changed. In fact, the equilibrium baroclinic response can be quite large because the anomalous meridional heat transport can only be balanced by slow radiative restoration in the absence of eddy feedbacks (not shown).

Things are very different however when eddy feedbacks are allowed. We focus on the effect of the baroclinic forcing by considering the full-model response when forcing with equal torques of opposite sign in the interior ( $\sigma_0 = 0.45$ ) and near the surface ( $\sigma_0 = 0.85$ ). To the extent that the full response is linear, this may be regarded as the difference between the responses to an interior and a near-surface torque at the same latitude.

Figure 8 shows the EP flux response when this dipolar structure is located on either the poleward or the equatorward flank of the jet. We can see that in both cases the anomalous westerly torque in the interior is roughly balanced by anomalous EP flux convergence and the anomalous easterly torque near the surface by anomalous EP flux divergence. Moreover, the anomalous EP convergence results almost entirely from the vertical component, so that the imposed baroclinic forcing is balanced locally and the response is negligible at other latitudes. What this implies is that the strong negative feedback by the eddy heat flux prevents the large changes in baroclinicity predicted by the zonally symmetric model. The strong eddy feedback against changes in baroclinicity is consistent with baroclinic adjustment and related theories (Schneider 2004; Zurita-Gotor 2008). As a result of this feedback, the response to a prescribed torque is only weakly sensitive on the

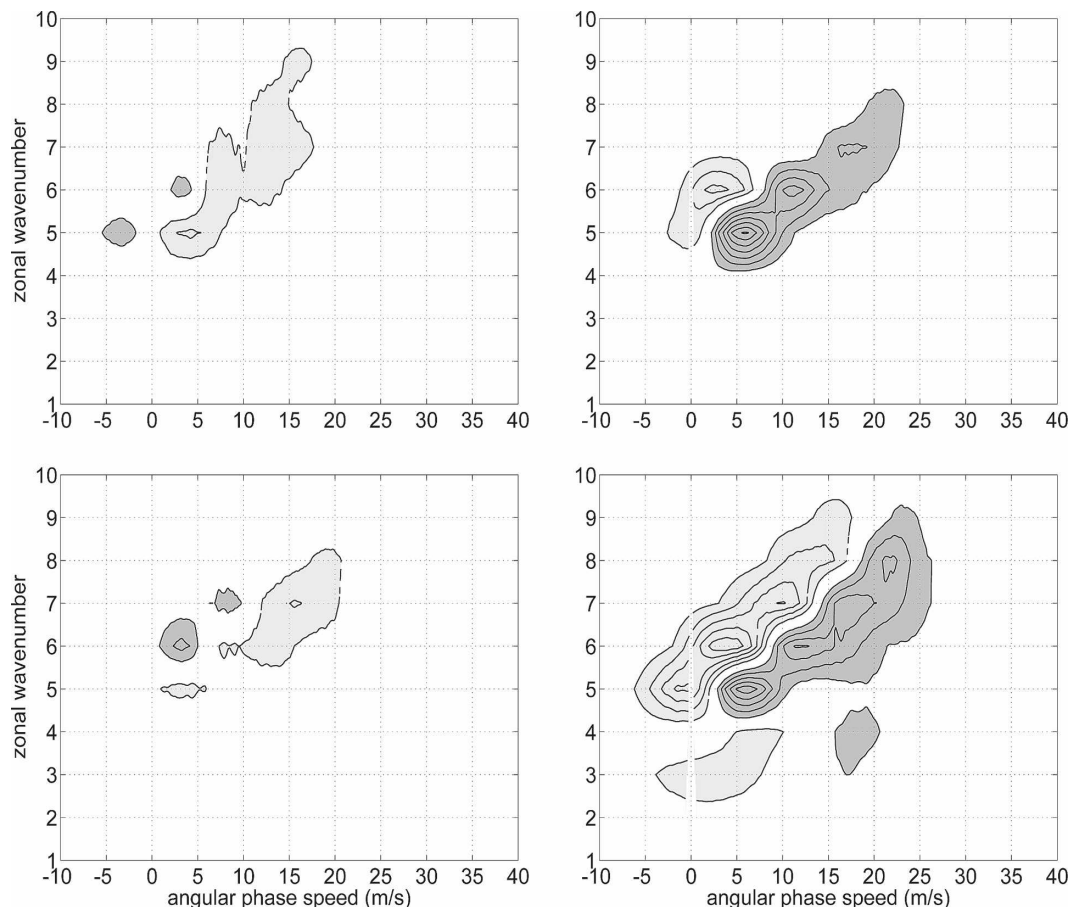


FIG. 7. The changes in the zonal wavenumber–phase speed spectra of the (top) upper-level ( $\sigma = 0.230$ ) eddy momentum flux and (bottom) lower-level ( $\sigma = 0.843$ ) eddy heat flux, for the same surface torques on the jet’s (left) equatorward flank and (right) poleward flank as in Fig. 4. The momentum flux is area averaged between  $35^\circ$  and  $45^\circ$ , and the heat flux is averaged between  $45^\circ$  and  $55^\circ$ . The contour intervals are  $0.007 \text{ m}^2 \text{ s}^{-2}$  for the momentum flux and  $0.01 \text{ K m s}^{-1}$  for the heat flux. The dark (light) shading denotes positive (negative) values.

forcing level, and remains quite barotropic even when the torque is moved to the upper troposphere (Fig. 3).

**5. Response to the stratospheric forcing**

We study the stratospheric influence on the troposphere by considering again two experiments in which the lower-stratosphere ( $\sigma_0 = 0.056$ ) zonal torques are located in the subtropics ( $\phi_0 = 30$ ) and high latitudes ( $\phi_0 = 70$ ). Figure 9 shows the time and zonally averaged changes in the zonal wind and EP flux divergence. In both cases, the westerly torque leads to a zonal wind increase that penetrates downward into the troposphere. However, this penetration is not vertical as is the case for the upper-troposphere torque but rather displays a slope that is different for each case. There is a poleward tilt for the subtropical torque, an equatorward tilt for the high-latitude torque, and less tilting for

midlatitude torques (not shown). The slope of the zonal wind response also agrees with the directions of anomalous wave propagation. Since the structure of the response is different in the three cases, it is not very meaningful to describe the stratospheric response in terms of its projection on the internal mode.

On the other hand, the tropospheric response to the stratospheric torque still displays the familiar annular mode structure described in previous sections, with one important difference: the sign of the response no longer depends on the forcing latitude. This is not surprising because the tilting of the zonal wind change is such that, in the troposphere, the westerly acceleration occurs roughly at the same latitudes for both forcings. This tropospheric pattern is consistent with an increase in the eddy phase speed and a poleward displacement of the jet. Westerly wind anomalies are again also seen in the upper troposphere as the subtropical jet strengthens

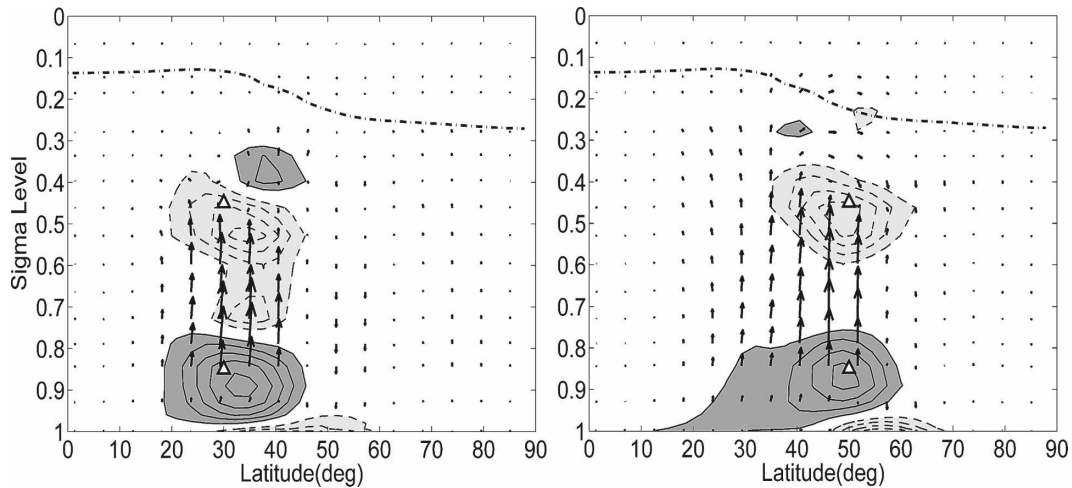


FIG. 8. The EP flux divergence difference for zonal torques in the tropospheric interior ( $\sigma_0 = 0.45$ ) and near the surface ( $\sigma_0 = 0.85$ ), which are placed on the jet's (left) equatorward flank and (right) poleward flank. The triangular symbols mark the locations of the anomalous westerly torque in the interior and the anomalous easterly torque near the surface. The contour intervals are  $0.5 \text{ m s}^{-1} \text{ day}^{-1}$  for the EP flux divergence, and  $4 \text{ m s}^{-1} \text{ day}^{-1}$  ( $\Delta\sigma, \Delta\phi$ ) for the EP vectors. Note that the vertical scale is linear in the plots.

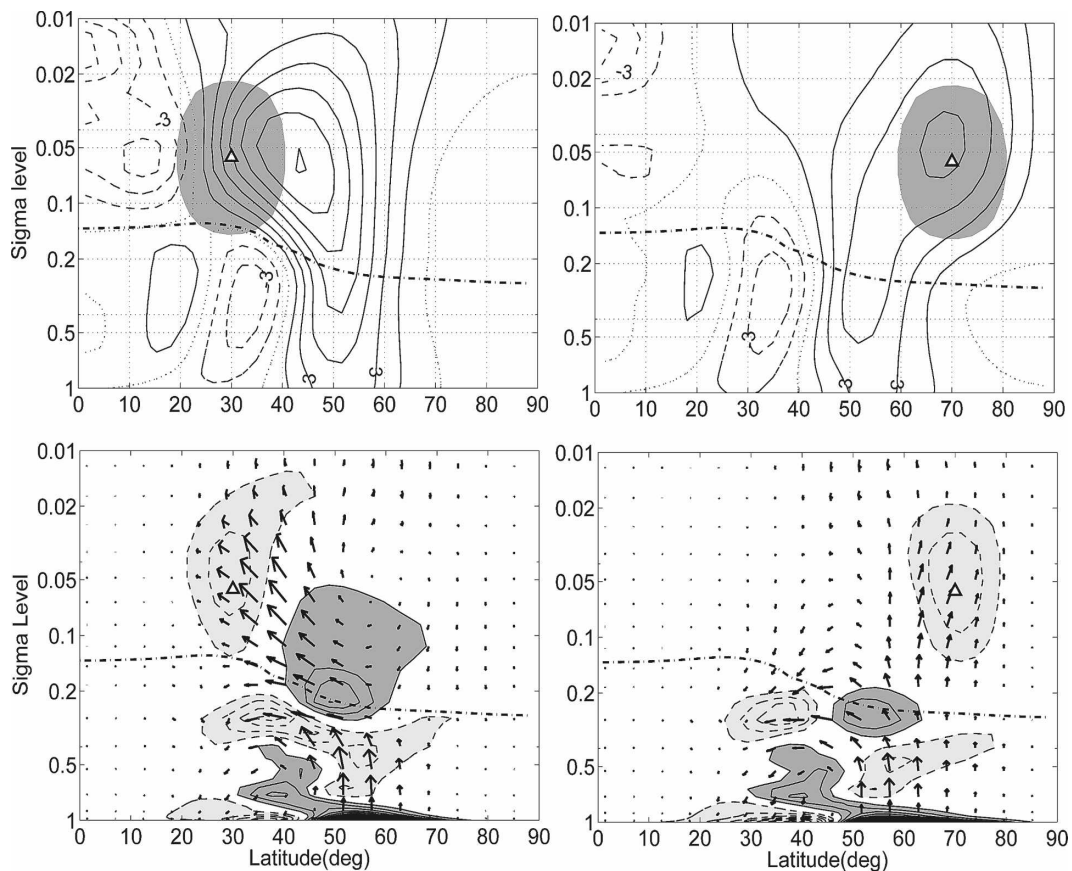


FIG. 9. The time and zonally averaged changes in the (top) zonal wind and (bottom) EP flux divergence for zonal torques in the lower stratosphere ( $\sigma_0 = 0.056$ ), which are placed in the (left) subtropics ( $\phi_0 = 30$ ) and (right) high latitudes ( $\phi_0 = 70$ ). The triangular symbol denotes the forcing center, and the shading in the top panels denotes the region where the torque is greater than  $0.5 \text{ m s}^{-1} \text{ day}^{-1}$ . The contour intervals are  $1.5 \text{ m s}^{-1}$  for the zonal wind,  $0.5 \text{ m s}^{-1} \text{ day}^{-1}$  for the EP flux divergence, and  $4 \text{ m s}^{-1} \text{ day}^{-1}$  ( $\Delta\sigma, \Delta\phi$ ) for the EP vectors.

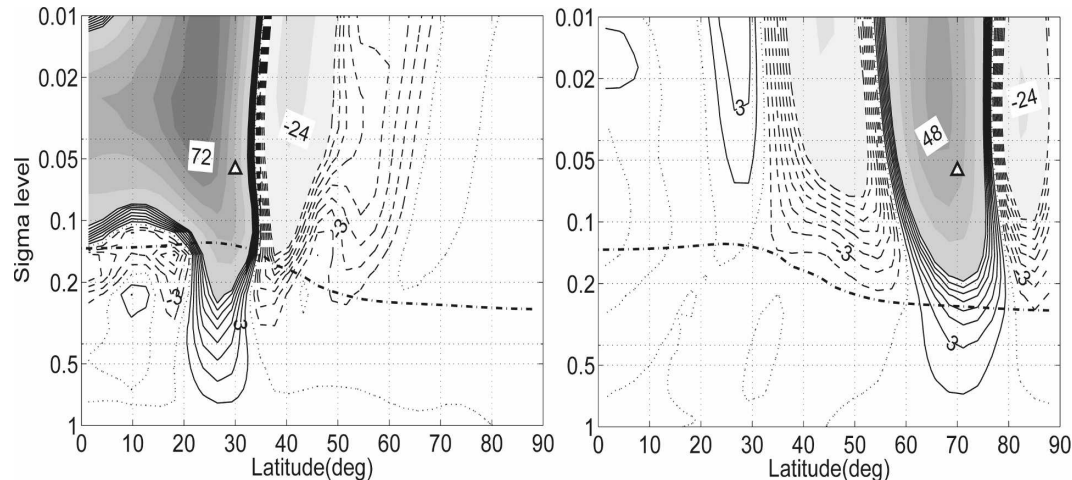


FIG. 10. The zonal wind changes in the zonally symmetric model for the same lower-stratospheric torques in the (left) subtropics and (right) high latitudes as in Fig. 9. The triangular symbol denotes the forcing center. The dashed-dotted lines in the plots are the tropopause level in the control simulation. The zonal wind changes are denoted by the shading with an interval of  $12 \text{ m s}^{-1}$ , and by the contours with an interval of  $1.5 \text{ m s}^{-1}$  for values less than  $12 \text{ m s}^{-1}$ .

and gets detached from the poleward-displaced eddy-driven jet.

The response to a stratospheric forcing cannot simply be thought of as a zonally symmetric balance with surface friction plus tropospheric eddy feedbacks. This can be easily seen in the zonal wind responses for the lower-stratospheric torques in the zonally symmetric model in Fig. 10. The zonal wind changes are a factor of 8 stronger than those in the full model, and the downward penetrations of the zonal winds are vertical. In particular, the downward penetration for the subtropical torque is such that, in the presence of tropospheric eddy feedbacks, it would lead to a jet shift in the opposite direction to that in the full model. These results suggest that the stratospheric eddies are important not only for the magnitude of the stratospheric response, but also for the direction of the tropospheric jet shift. One can think of the tropospheric response as resulting from the tropospheric eddy feedback on a mean flow that is modified not just by the prescribed torque, but also by the stratospheric eddies.

We extract the effects of the stratospheric eddies by removing the projections of the model responses on the internal annular mode with the least square regression in Eq. (4). Figure 11 shows the resulting residual pattern in the zonal wind and EP flux divergence, compared with the EP flux divergence response due to planetary waves alone ( $m \leq 3$ ). The residual wave activity displays a pattern in which anomalous waves originate from the surface, propagate vertically across the tropopause, and converge into the regions of the

stratospheric westerly torque. (Note that such a clear residual wave activity pattern can be obtained only if the imposed torque is separated from the tropospheric annular mode.) We refer to this residual pattern as the “stratospheric eddy response.” A comparison with the full response shows that the stratospheric eddy response is primarily due to planetary waves for the subtropical forcing, but is dominated by medium-scale waves for the subtropical forcing. The net effect of the prescribed forcing and the stratospheric eddies is to increase the zonal winds mostly in the stratosphere. While the wave activity residual includes some tropospheric eddies, more experiments with the zonally symmetric model confirm that the stratospheric eddies alone can generate similar zonal wind changes in the stratosphere (not shown), as is also seen in Kushner and Polvani (2004).

Despite the increased upward EP flux across the tropopause, we argue that the increased lower-stratospheric wind is the key for the tropospheric jet shift. The lower-stratospheric wind shears can alter the baroclinic eddy life cycle in the troposphere through changes in the phase speed of the tropospheric eddies (Wittman et al. 2007). As stratospheric signals are transmitted downward by planetary waves mainly through the midlatitude tropopause on the poleward flank of the tropospheric jet (Fig. 9), it seems plausible that the stratospheric westerly torque can accelerate the phase speed of the tropospheric eddies. The only exception is the torque in low latitudes far away from stratospheric eddies ( $\phi_0 = 20^\circ$ ,  $\sigma_0 = 0.056$ ). We have

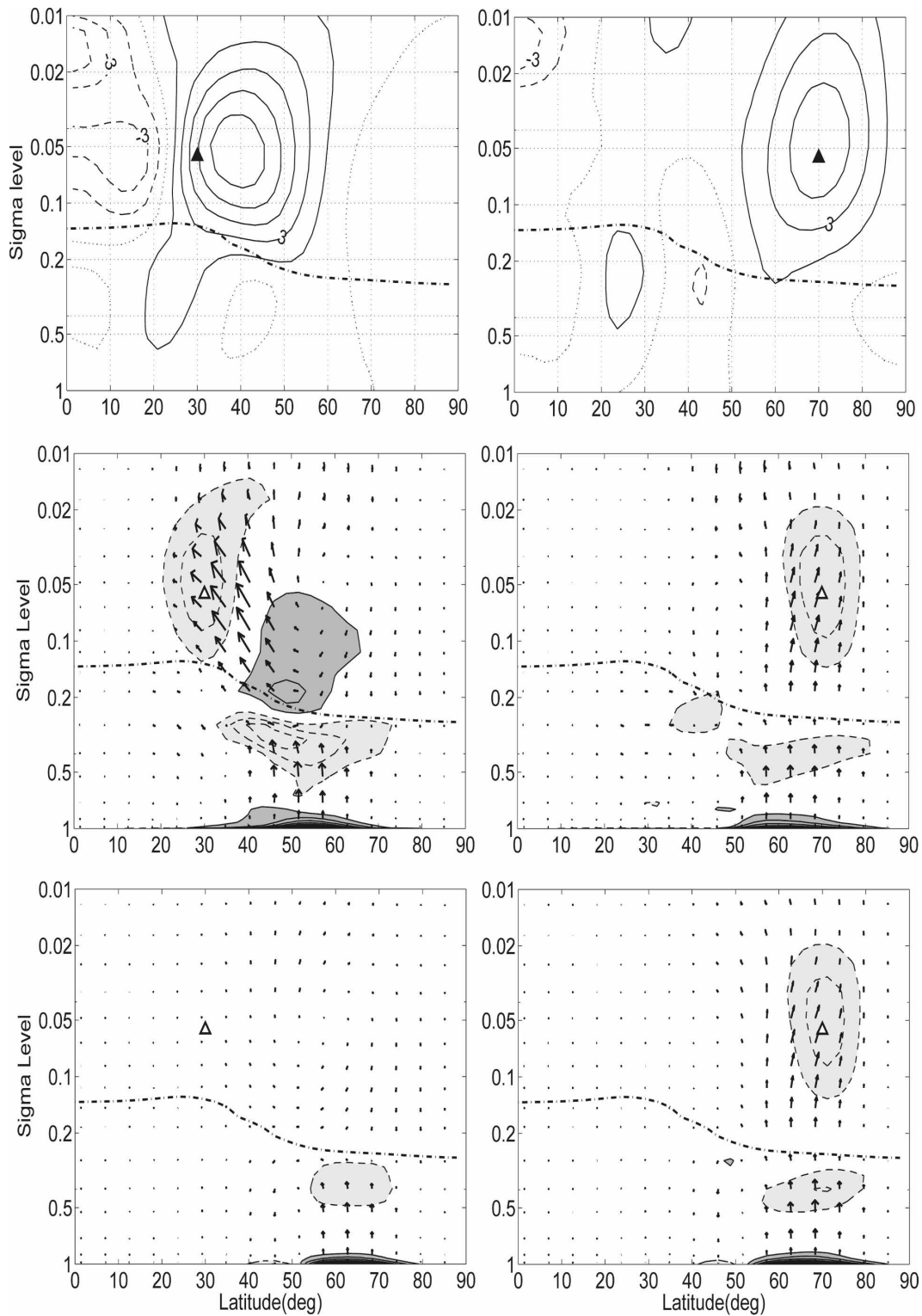


FIG. 11. The residual patterns obtained by removing the annular mode projection in the (top) zonal wind and (middle) EP flux divergence, in comparison with (bottom) the responses in the EP flux divergence due to the planetary waves ( $m \leq 3$ ), for the same lower stratospheric torques in the (left) subtropics and (right) high latitudes as in Fig. 9. The contour intervals are  $1.5 \text{ m s}^{-1}$  for the zonal wind,  $0.5 \text{ m s}^{-1} \text{ day}^{-1}$  for the EP flux divergence, and  $4 \text{ m s}^{-1} \text{ day}^{-1}$  ( $\Delta\sigma$ ,  $\Delta\phi$ ) for the EP vectors.

also examined the latitude–phase speed spectra and wavenumber–phase speed spectra of the upper-level eddy momentum flux and lower-level eddy heat flux responses (not shown). These spectra are remarkably similar to those for a tropospheric torque on the poleward flank of the jet, displaying increases in the phase speed of midlatitude eddies for both eddy fluxes. As such, the lower-stratospheric wind anomalies can be thought to project onto the tropospheric annular mode.

Like the upper-tropospheric torque, the eddy fluxes play an important role in balancing the stratospheric torque; however, the dynamics is more complex now because meridional wave propagation in the stratosphere is also important. This is also different from a balance by residual circulations, which penetrates downward vertically. In our model, waves enter the stratosphere primarily through the middle- and high-latitude tropopause. Since waves are only forced by baroclinic instability and upscale nonlinear transport in our model, there is not a significant long-wave spectrum in the midlatitudes. It is thus possible that the response to a stratospheric torque would be more complicated in a model with midlatitude planetary wave forcing.

As the torque is moved aloft in the stratosphere, the eddies are less efficient in balancing the torque and the meridional circulations become more important. Figure 12 shows the time and zonally averaged responses in the zonal wind, EP flux divergence, and the Coriolis deceleration of the meridional residual circulation for a zonal torque in the subtropical middle stratosphere ( $\phi_0 = 30^\circ$ ,  $\sigma_0 = 0.01$ ). In contrast to the lower-stratospheric torque in Fig. 9, the middle-stratospheric torque is mainly balanced at the center by the Coriolis deceleration because of anomalous equatorward residual circulation, and this results in very intense zonal winds at the forcing center. There also exists anomalous equatorward wave propagation at the forcing level that attempts to reduce the meridional shears of the zonal winds, which might be related to barotropic instability in the stratosphere. Despite these differences, the influence on the troposphere shows the same characteristics as before, with the zonal wind response again tilting poleward and anomalous upward wave propagation from the middle- and high-latitude tropopause into the torque region. This suggests that the stratospheric eddies still control the direction of the tropospheric jet shift, rather than the strong meridional circulations. These stratospheric eddies transfer positive zonal wind anomalies down to the tropopause level on the poleward flank of the jet, and project onto the positive phase of the tropospheric annular mode.

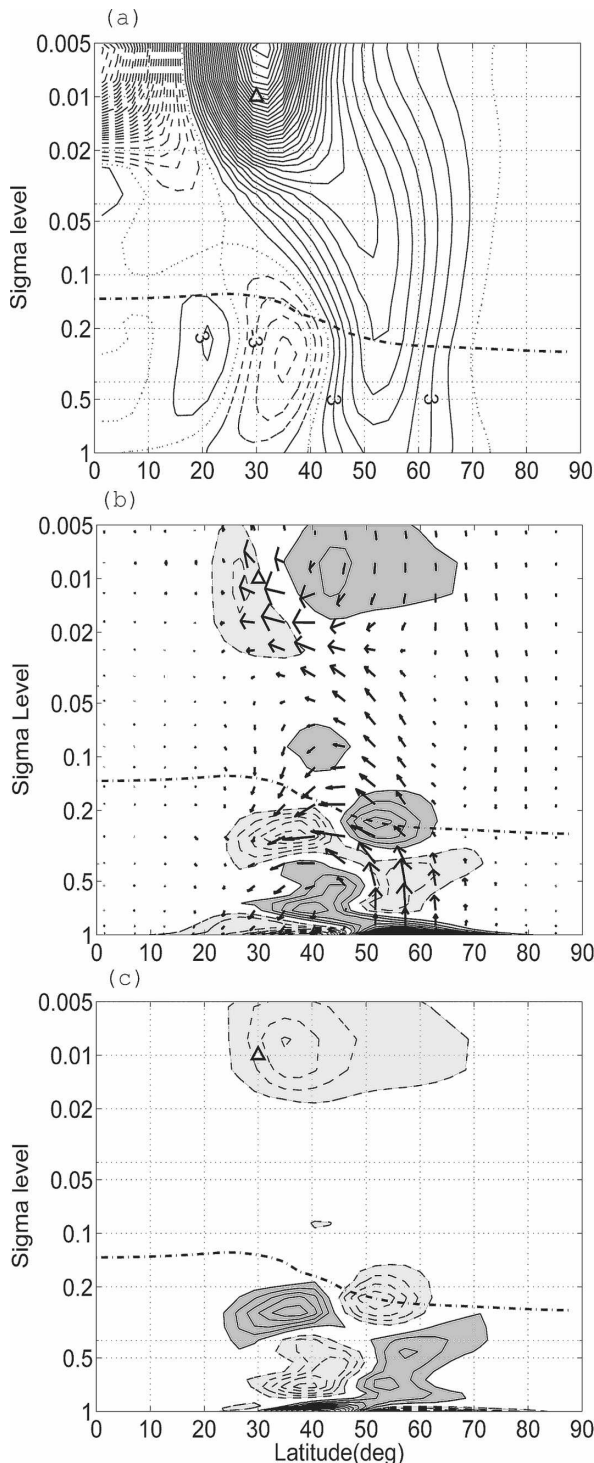


FIG. 12. The time and zonally averaged responses in (a) the zonal wind, (b) the EP flux divergence, and (c) the Coriolis deceleration of the meridional residual circulation for the zonal torque in the subtropical middle stratosphere ( $\phi_0 = 30^\circ$ ,  $\sigma_0 = 0.01$ ). The triangular symbol denotes the forcing center. The contour intervals are  $1.5 \text{ m s}^{-1}$  for the zonal wind,  $0.5 \text{ m s}^{-1} \text{ day}^{-1}$  for the EP flux divergence and the Coriolis deceleration, and  $4 \text{ m s}^{-1} \text{ day}^{-1}$  ( $\Delta\sigma$ ,  $\Delta\phi$ ) for the EP vectors.

## 6. The jet response to the orographic GWD parameterization

In this section, we discuss the implications of our results for the orographic GWD parameterization using GFDL climate model AM2.1. AM2.1 is a global atmosphere and land model forced by the observed values of radiative forcing agents, sea surface temperatures, and sea ice (GFDL Global Atmospheric Model Development Team 2004) that is integrated from January 1983 to December 1998 for this study. The model uses the GWD parameterization described in Stern and Pierrehumbert (1988), in which the GWD is deposited at the level where the momentum flux transferred from below exceeds the saturation flux. The surface momentum flux  $\tau_s$  is parameterized as

$$\tau_s \propto U^3 G^* \frac{F^2}{F^2 + a^2}, \quad (5)$$

where  $U$  is the surface wind;  $F$  is the Froude number, which is a function of surface orography; and  $G^*$  and  $a$  are two nondimensional constants that are both tuned to a value of 1 to optimize the simulated zonal mean winds. We change the parameter  $G^*$  in our sensitivity study, which results in a change in the parameterized momentum flux at the surface and the gravity wave drag deposited in the lower stratosphere.

Figure 13 shows the 16-yr wintertime (December–February, DJF) and zonal mean zonal wind in the control experiment in which  $G^* = 1.0$ , and the zonal wind response as  $G^*$  is reduced from 1.5 to 0.5. We also show the regression of the zonal wind anomaly onto the standardized Northern Hemisphere annular mode index, defined as the first principal component of the monthly DJF sea level pressure field poleward of  $20^\circ\text{N}$  in the control experiment. Despite the amplitude difference, the regression pattern simulated in the model resembles the annular mode structure in the observations. The GWD in the model is mainly deposited above the subtropical jet core in the lower stratosphere. The decreased easterly drag leads to an increase in the zonal wind, which penetrates downward and poleward, and projects onto the internal annular mode only in the troposphere. The zonal wind change is similar to the response to the subtropical stratospheric torque in the idealized model (Fig. 9). This suggests that the stratospheric polar vortex is not fundamental for the downward influence, although it may still play an important role in the vertical propagation of planetary waves. The same is true for the case of a high-latitude torque, as the downward and equatorward penetration of the zonal wind in our model also resembles that in SR and the observed zonal wind change associated with

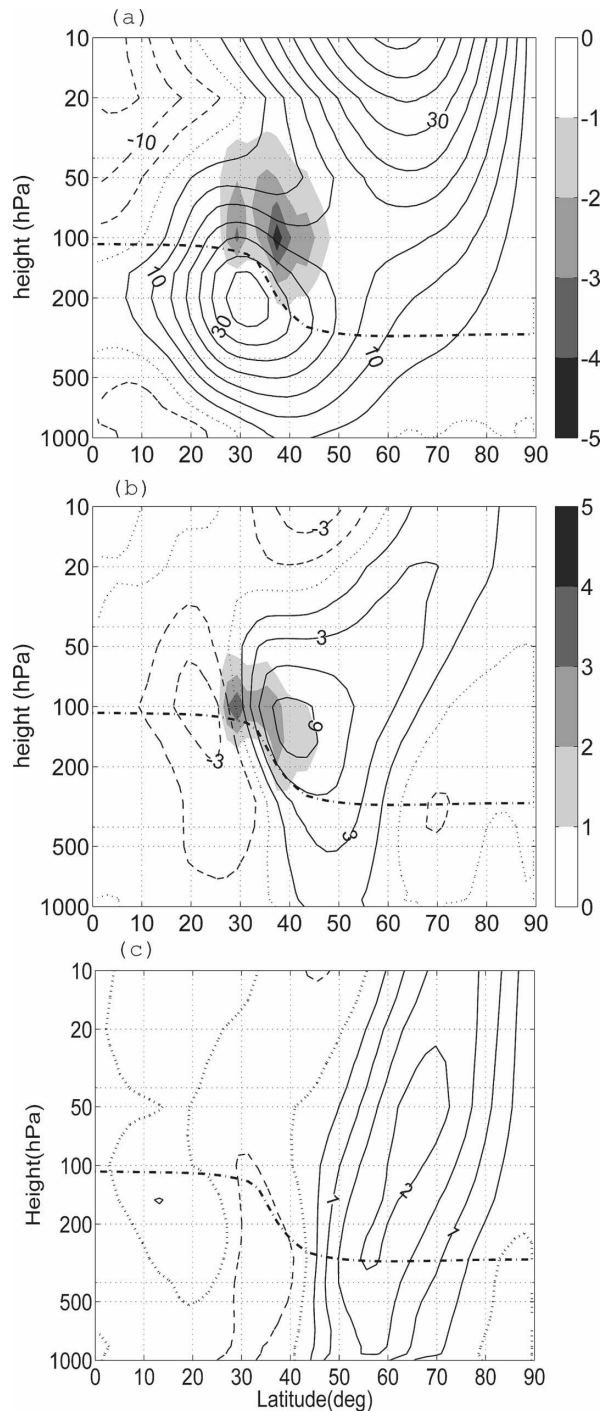


FIG. 13. The 16-yr wintertime (DJF) and zonally averaged (a) zonal wind in the control experiment in which  $G^* = 1.0$ , (b) the zonal wind response as  $G^*$  is reduced from 1.5 to 0.5, and (c) the regression of the zonal wind anomaly onto the standardized Northern Hemisphere annular mode index in the control experiment in the GFDL AM2.1. Here,  $G^*$  is the GWD parameter, with a larger value denoting stronger zonal wind deceleration. The shading in (a) and (b) denotes the zonal wind acceleration by GWD, with an interval of  $1 \text{ m s}^{-1} \text{ day}^{-1}$ . The contour intervals are  $5 \text{ m s}^{-1}$  for (a),  $1.5 \text{ m s}^{-1}$  for (b), and  $0.5 \text{ m s}^{-1}$  for (c).

anomalous stratospheric wave drag (e.g., Black 2002; Thompson et al. 2006). These results suggest that our understandings from the idealized model may also be relevant for the tropospheric jet shift in response to the stratospheric forcing, even when a stratospheric polar jet exists.

The tropospheric jet sensitivity in Fig. 3 implies that the level of gravity wave breaking may have a considerable impact on the tropospheric jet latitude. First, if some of the GWD were deposited below the tropopause level, the tropospheric jet would shift poleward, with little dependence on the drag profile in the troposphere, consistent with Stephenson (1994). On the other hand, if the gravity wave breaking were to occur at a higher level in the stratosphere, the decreased air density would result in a greater zonal wind deceleration so as to satisfy angular momentum conservation, and therefore we should anticipate a more dramatic jet shift (associated with the increased forcing amplitude) than is seen in Fig. 3.

We have also looked at the spatial distribution in the surface wind response (not shown). Although the GWD in the lower stratosphere is localized over steep topography, the surface wind response displays a zonally symmetric component; that is, the surface westerlies are displaced poleward in both the Atlantic and Pacific Oceans. This surface wind response is very similar to the internal annular mode pattern, justifying that our understandings from a model with zonally symmetric lower boundary conditions are relevant to GCMs with more complex boundary conditions.

## 7. Discussion and conclusions

We study the tropospheric response to prescribed zonal forcing in an idealized dry model. The tropospheric jet shifts equatorward for a westerly (eastward) zonal torque on the equatorward flank of the jet in the troposphere. In contrast, the tropospheric jet moves poleward for a torque on the poleward flank of the jet in the troposphere, and for a torque in the extratropical stratosphere. These jet movements project strongly onto the internal annular mode in the troposphere.

These jet movements can be explained based on the changes in the critical latitudes of tropospheric eddies. For a westerly torque near the surface, the response can be thought of as a zonally symmetric balance between the torque and surface friction at first (with surface winds modified until the increased surface friction balances the torque). The zonally symmetric response in the zonal wind is nearly barotropic above the forcing. This zonal wind change can have different impacts on eddies in the midlatitude region of baroclinic growth

versus the subtropical region of barotropic decay. While the increased zonal winds in the subtropics allow the midlatitude eddies to propagate farther into the tropics and result in the equatorward shift in the critical latitudes, the increased winds in the midlatitudes accelerate the eastward eddy phase speeds and lead to the poleward shift in the critical latitudes. Finally, as the torque is moved into the tropospheric interior, the eddy fluxes redistribute momentum vertically, producing a zonal wind response that is still nearly barotropic.

For the torque in the stratosphere, the stratospheric eddies play a more important role in controlling the tropospheric jet latitude than the residual circulations. Despite the lack of the stratospheric polar jet in this idealized model, the tropospheric response to the prescribed stratospheric forcing is similar to that in models with a more realistic stratosphere. The downward penetration of zonal winds to the troposphere displays a poleward slope for the subtropical torque, an equatorward slope for the high-latitude torque, and less tilting for the midlatitude torques. These slopes are the signatures of anomalous wave propagation in the stratosphere, in contrast to the vertical downward penetration, assuming that only the residual circulation changes. As the tropospheric eddies enter the stratosphere through the middle- and high-latitude tropopause, they transfer positive zonal wind anomalies from the torque region to the midlatitude lower stratosphere. We argue that these wind anomalies modify the eddy phase speeds in the upper troposphere, and displace the tropospheric jet as in the case of tropospheric forcing. However, further research is necessary to investigate how the stratospheric planetary-scale eddies interact at the tropopause level with the tropospheric medium-scale eddies. Such interactions are also observed, although not fully understood, in the life cycle of sudden stratospheric warming (e.g., Limpasuvan et al. 2004).

Concerned about the resolution dependence of the low-frequency variability in this type of model (Gerber et al. 2008), we have performed the control simulation and four experiments studied in sections 4 and 5 at higher horizontal resolution (T85) with the vertical resolution unchanged. The high-resolution runs produce qualitatively similar annular mode-like responses in the troposphere, and similar tilting structures of zonal winds in the stratosphere for the stratospheric torques (not shown). However, the decorrelation time scales of the annular modes in these experiments drop between 20 and 30 days, a range about the true time scale for the low-frequency variability in this model system (Gerber et al. 2008). This is approximately four times shorter than the time scales in the T42 simulations, and the tropospheric annular mode responses at

T85 are about three times smaller in magnitude than those at T42, which may be related to the fluctuation–dissipation theorem introduced by Leith (1975; E. Gerber and A. Plumb 2007, personal communication).

*Acknowledgments.* We are especially thankful to Isaac Held for his comments and suggestions. We are also grateful for valuable discussions with Alan Plumb, Lorenzo Polvani, Walter Robinson, Edwin Gerber, and Michael Ring. We thank three anomalous reviewers for helpful comments, and Bruce Wyman and S. J. Lin for integrating the GCM experiments. The lead author is supported by a NOAA Climate and Global Change Postdoctoral Fellowship, administered by the University Corporation for Atmospheric Research, and most of the work was done when he was a graduate student at Princeton University, supported by Award NA17RJ2612 from the National Oceanic and Atmospheric Administration, U.S. Department of Commerce. PZG is supported by the Ramon y Cajal program of the Ministerio de Educación y Ciencia of Spain and by a Universidad Complutense-Flores Valles fellowship.

#### REFERENCES

- Baldwin, M. P., and T. J. Dunkerton, 1999: Propagation of the Arctic Oscillation from the stratosphere to the troposphere. *J. Geophys. Res.*, **104**, 30 937–30 946.
- , and —, 2001: Stratospheric harbingers of anomalous weather regimes. *Science*, **294**, 581–584, doi:10.1126/science.1063315.
- Black, R. X., 2002: Stratospheric forcing of surface climate in the Arctic Oscillation. *J. Climate*, **15**, 268–277.
- Chang, E. K. M., 1995: The influence of Hadley circulation intensity changes on extratropical climate in an idealized model. *J. Atmos. Sci.*, **52**, 2006–2024.
- , 1998: Poleward-propagating angular momentum perturbations induced by zonally symmetric heat sources in the tropics. *J. Atmos. Sci.*, **55**, 2229–2248.
- Chen, G., and I. M. Held, 2007: Phase speed spectra and the recent poleward shift of Southern Hemisphere surface westerlies. *Geophys. Res. Lett.*, **34**, L21805, doi:10.1029/2007GL031200.
- , —, and W. A. Robinson, 2007: Sensitivity of the latitude of the surface westerlies to surface friction. *J. Atmos. Sci.*, **64**, 2899–2915.
- Chen, P., and W. A. Robinson, 1992: Propagation of planetary waves between the troposphere and stratosphere. *J. Atmos. Sci.*, **49**, 2533–2545.
- Gerber, E. P., S. Voronin, and L. M. Polvani, 2008: Testing the annular mode autocorrelation time scale in simple atmospheric general circulation models. *Mon. Wea. Rev.*, **136**, 1523–1536.
- GFDL Global Atmospheric Model Development Team, 2004: The new GFDL global atmosphere and land model AM2/LM2: Evaluation with prescribed SST simulations. *J. Climate*, **17**, 4641–4673.
- Haigh, J. D., M. Blackburn, and R. Day, 2005: The response of tropospheric circulation to perturbations in lower-stratospheric temperature. *J. Climate*, **18**, 3672–3685.
- Hartmann, D. L., and P. Zuercher, 1998: Response of baroclinic life cycles to barotropic shear. *J. Atmos. Sci.*, **55**, 297–313.
- Haynes, P. H., C. J. Marks, M. E. McIntyre, T. G. Shepherd, and K. P. Shine, 1991: On the “downward control” of extratropical diabatic circulations by eddy-induced mean zonal forces. *J. Atmos. Sci.*, **48**, 651–678.
- Held, I. M., and P. J. Phillips, 1987: Linear and nonlinear barotropic decay on the sphere. *J. Atmos. Sci.*, **44**, 200–207.
- , and M. J. Suarez, 1994: A proposal for the intercomparison of the dynamical cores of atmospheric general circulation models. *Bull. Amer. Meteor. Soc.*, **75**, 1825–1830.
- Kushner, P. J., and L. M. Polvani, 2004: Stratosphere–troposphere coupling in a relatively simple AGCM: The role of eddies. *J. Climate*, **17**, 629–639.
- Leith, C. E., 1975: Climate response and fluctuations. *J. Atmos. Sci.*, **32**, 2022–2026.
- Limpasuvan, V., D. W. J. Thompson, and D. L. Hartmann, 2004: The life cycle of the Northern Hemisphere sudden stratospheric warmings. *J. Climate*, **17**, 2584–2596.
- Norton, W. A., 2003: Sensitivity of Northern Hemisphere surface climate to simulation of the stratospheric polar vortex. *Geophys. Res. Lett.*, **30**, 1627, doi:10.1029/2003GL016958.
- Perlwitz, J., and N. Harnik, 2003: Observational evidence of a stratospheric influence on the troposphere by planetary wave reflection. *J. Climate*, **16**, 3011–3026.
- Polvani, L. M., and P. J. Kushner, 2002: Tropospheric response to stratospheric perturbations in a relatively simple general circulation model. *Geophys. Res. Lett.*, **29**, 1114, doi:10.1029/2001GL014284.
- Randel, W. J., and I. M. Held, 1991: Phase speed spectra of transient eddy fluxes and critical layer absorption. *J. Atmos. Sci.*, **48**, 688–697.
- Ring, M. J., and R. A. Plumb, 2007: Forced annular mode patterns in a simple atmospheric general circulation model. *J. Atmos. Sci.*, **64**, 3611–3626.
- Robinson, W. A., 1997: Dissipation dependence of the jet latitude. *J. Climate*, **10**, 176–182.
- , 2000: A baroclinic mechanism for the eddy feedback on the zonal index. *J. Atmos. Sci.*, **57**, 415–422.
- , 2002: On the midlatitude thermal response to tropical warmth. *Geophys. Res. Lett.*, **29**, 1190, doi:10.1029/2001GL014158.
- Scaife, A. A., J. R. Knight, G. K. Vallis, and C. K. Folland, 2005: A stratospheric influence on the winter NAO and North Atlantic surface climate. *Geophys. Res. Lett.*, **32**, L18715, doi:10.1029/2005GL023226.
- Schneider, T., 2004: The tropopause and thermal stratification in the extratropics of a dry atmosphere. *J. Atmos. Sci.*, **61**, 1317–1340.
- Scott, R. K., and L. Polvani, 2006: Internal variability of the winter stratosphere. Part I: Time-independent forcing. *J. Atmos. Sci.*, **63**, 2758–2776.
- Seager, R., N. Harnik, Y. Kushnir, W. Robinson, and J. Miller, 2003: Mechanisms of hemispherically symmetric climate variability. *J. Climate*, **16**, 2960–2978.
- Simmons, A. J., and B. J. Hoskins, 1980: Barotropic influences on the growth and decay of nonlinear baroclinic waves. *J. Atmos. Sci.*, **37**, 1679–1684.
- , and D. M. Burridge, 1981: An energy and angular-momentum conserving vertical finite-difference scheme and hybrid vertical coordinates. *Mon. Wea. Rev.*, **109**, 758–766.
- Son, S. W., and S. Lee, 2005: The response of westerly jets to

- thermal driving in a primitive equation model. *J. Atmos. Sci.*, **62**, 3741–3757.
- Song, Y., and W. A. Robinson, 2004: Dynamical mechanisms for stratospheric influences on the troposphere. *J. Atmos. Sci.*, **61**, 1711–1725.
- Stephenson, D. B., 1994: The Northern Hemisphere tropospheric response to changes in the gravity-wave drag scheme in a perpetual January GCM. *Quart. J. Roy. Meteor. Soc.*, **120**, 699–712.
- Stern, W. F., and R. T. Pierrehumbert, 1988: The impact of an orographic gravity wave drag parameterization on extended range predictions with a GCM. Preprints, *Eighth Conf. on Numerical Weather Prediction*, Baltimore, MD, Amer. Meteor. Soc., 745–750.
- Taguchi, M., 2003: Tropospheric response to stratospheric degradation in a simple global circulation model. *J. Atmos. Sci.*, **60**, 1835–1846.
- Thompson, D. W. J., and S. Solomon, 2002: Interpretation of recent Southern Hemisphere climate change. *Science*, **296**, 895–899.
- , M. P. Baldwin, and S. Solomon, 2005: Stratosphere–troposphere coupling in the Southern Hemisphere. *J. Atmos. Sci.*, **62**, 708–715.
- , J. C. Furtado, and T. G. Shepherd, 2006: On the tropospheric response to anomalous stratospheric wave drag and radiative heating. *J. Atmos. Sci.*, **63**, 2616–2629.
- Thorncroft, C. D., B. J. Hoskins, and M. E. McIntyre, 1993: Two paradigms of baroclinic wave life-cycle behaviour. *Quart. J. Roy. Meteor. Soc.*, **119**, 17–55.
- Wittman, M., L. M. Polvani, and A. J. Charlton, 2007: The effect of lower-stratospheric shear on baroclinic instability. *J. Atmos. Sci.*, **64**, 479–496.
- Zurita-Gotor, P., 2008: The sensitivity of the isentropic slope in a primitive equation dry model. *J. Atmos. Sci.*, **65**, 43–65.